Journal of Nano- and Electronic Physics
Vol. **17** No 3, 03029(9pp) (2025)

Журнал нано- та електронної фізики
Том **17** № 3, 03029(9cc) (2025)

REGULAR ARTICLE

Enhancing Concentrated Solar Photovoltaic (CSPV) Efficiency through Co-Doped ZnO Window Layers and Bi-As Infused GaSb Substrates

Charef Azzeddine[1,2,*], Karima Zitouni[1], Said Benramache[2],
Khattra Mimouni[1], Abderrahmane Kadri[1]

[1] *LEMOP Laboratory, Laboratoire d'Etude des Matériaux Optoélectronique et Polymères,University Oran1, Algeria*
[2] *Laboratoire de Physique Photonique et Nanomatériaux Multifonctionnels, LPPNM, Biskra University, Algeria*

(Received 22 February 2025; revised manuscript received 20 June 2025; published online 27 June 2025)

This study explores the performance enhancement of Concentrated Solar Photovoltaic (CSPV) modules through optimized oxide layers and a unique GaSb substrate infused with bismuth-arsenic compounds (Bi-As) to improve solar energy conversion. Two configurations were examined: one with a pure ZnO oxide window and another using Co-doped ZnO ($Zn_{0.94}Co_{0.06}O$). Both modules included GaSb layers enriched with 3 % and 6 % Bi in GaSbBi and GaAsSbBi, respectively, to increase light absorption.Results show a notable efficiency gain in the module with the $Zn_{0.94}Co_{0.06}O$ window, demonstrating its superior performance over the ZnO-based module regardless of the GaAsSbBi layer thickness. The CSPV module with ZnO achieved an energy conversion efficiency of 13.55 % and a fill factor (FF) of 76.42 %. In comparison, Co-doped ZnO ($Zn_{0.94}Co_{0.06}O$) significantly improved efficiency, reaching 15.89 % with an FF of 72.90 %.This increase in output underscores the effectiveness of Co-doped ZnO as an advanced window layer, boosting energy conversion efficiency consistently across various GaAsSbBi thicknesses. The findings indicate that the Co-doped ZnO oxide layer presents a promising approach for CSPV module optimization, making it a valuable development in enhancing photovoltaic efficiency and contributing to more sustainable solar energy solutions.

Keywords: CSPV modules, Co-doped ZnO, GaSbBi substrates, Solar efficiency optimization.

DOI: 10.21272/jnep.17(3).03029 PACS numbers: 88.40.jp –, 88.40.hj

1. INTRODUCTION

As global energy demands increase alongside concerns about environmental sustainability, renewable energy sources have become essential for sustainable development. Solar energy, in particular, has attracted considerable interest due to its vast availability and relatively low environmental impact [1]. Among various solar technologies, Concentrated Solar Photovoltaic (CSPV) systems stand out due to their ability to achieve high efficiency by focusing sunlight onto small areas of high-performance solar cells, thereby maximizing energy output while reducing material costs [2]. However, despite these advantages, CSPV systems still face significant challenges, especially at high concentration levels, where issues like excessive heat buildup, material degradation, and suboptimal light absorption hinder overall efficiency [3].

One promising approach to overcoming these challenges lies in optimizing the materials within CSPV modules, particularly in layers that impact light absorption and carrier collection. Zinc oxide (ZnO) has long been a popular choice for window layers in solar cells due to its favorable optical transparency and electron mobility [4]. However, recent research indicates that doping ZnO with cobalt (Co) can enhance its optical and electrical properties, making it even more effective as a window layer in CSPV modules [5].

By introducing cobalt into the ZnO matrix, the material's electronic properties are altered, potentially improving light absorption and enhancing charge transport, which reduces energy losses commonly encountered in the photovoltaic process [6]. In this study, we investigate how Co-doped ZnO (specifically $Zn_{0.94}Co_{0.06}O$) performs compared to undoped ZnO to determine if it can significantly enhance the energy output of CSPV cells [7].

In addition to exploring improved window materials, another area of innovation in CSPV technology involves the use of advanced substrate layers. Gallium antimonide (GaSb), a substrate material with promising electronic properties, can be infused with bismuth (Bi) and arsenic (As) to enhance light absorption across a broader spectrum [8]. When bismuth and arsenic are incorporated into GaSb, they modify the bandgap, enabling the material to capture photons across a wider range of wavelengths, including the infrared region [5]. This capability is especially valuable in CSPV modules, where absorbing additional light can translate directly into higher conversion efficiencies [5]. In our research, we specifically utilize GaSbBi and GaAsSbBi layers with Bi concentrations of 3 % and 6 %, respectively, to determine how varying thicknesses and compositions affect overall module performance [9].

The goal of this research is to systematically explore how Co-doped ZnO and GaSb-based substrates infused

---

[*] Correspondence e-mail: azzoucharef3@gmail.com

Cite this article as: C. Azzeddine, et al., *J. Nano- Electron. Phys.* 17 No 3, 03029 (2025) https://doi.org/10.21272/jnep.17(3).03029

with bismuth and arsenic can enhance CSPV module efficiency. By investigating the interactions between these materials, this study aims to provide insights into how CSPV systems can achieve greater output and stability, advancing toward more efficient and economically viable solar energy solutions [10].

2. COMPARISON OF CSPV CELL PERFORMANCE: ZNO VS. CO-DOPED ZNO WINDOW LAYERS

In the quest for enhancing the efficiency of Concentrated Solar Photovoltaic (CSPV) cells, material optimization plays a crucial role. This section presents a comparative analysis of two CSPV cell structures: one utilizing a traditional ZnO window layer and the other employing a Co-doped ZnO layer. By analyzing key performance metrics, including open-circuit voltage, short-circuit current density, fill factor, and overall efficiency, we aim to highlight the impact of Co-doping on solar cell performance and its potential to improve energy conversion in CSPV applications.

2.1 Diagram of the Solar Cell Structure 1: ZnO

Figure 1 illustrates the layered structure of the CSPV cell with a ZnO window layer, detailing the various materials and their respective thicknesses. Starting from the top, the cell features an aluminum (Al) contact layer, followed by an *n*-type ZnO layer with a thickness of 0.350 µm, which serves as the window layer, allowing light to enter the cell. Beneath it, there is an *n*-type GaAs layer, 0.150 µm thick, which contributes to efficient charge transport.

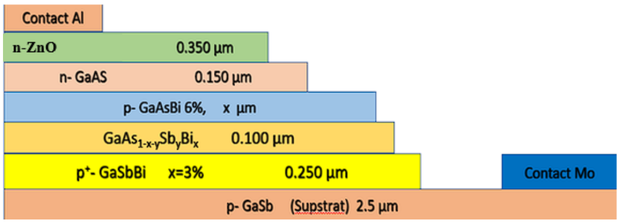

Fig. 1 – Layered structure diagram of the CSPV Cell with ZnO window layer

The structure continues with a *p*-type GaAsBi layer doped with 6 % bismuth, indicated with a variable thickness *x* µm. This layer is essential for enhancing absorption, particularly in the infrared spectrum. Below this, there is a $GaAs_{1-x-y}Sb_yBi_x$ layer with a fixed thickness of 0.100 µm, followed by another *p*-type GaSbBi layer with a 3 % bismuth concentration and a thickness of 0.250 µm, contributing to the light absorption process.

At the base of the cell, a *p*-type GaSb substrate, with a thickness of 2.5 µm, provides foundational support and further absorption capabilities. The structure concludes with a molybdenum (Mo) contact, which facilitates the collection of photogenerated charges. This carefully engineered layer configuration is designed to maximize light absorption and carrier collection, thereby enhancing the overall efficiency of the CSPV cell.

2.2 Diagram of the Solar Cell Structure 2: Co-doped ZnO

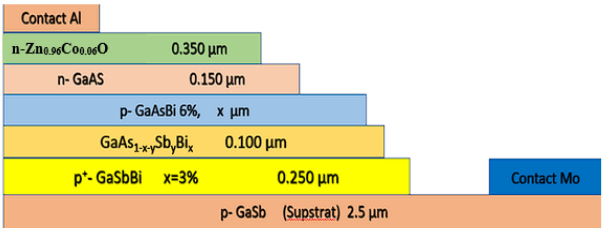

Fig. 2 – Layered structure diagram of the CSPV cell with ZnCoO window layer

Figure 2 depicts the layered structure of the CSPV cell utilizing a Co-doped ZnO ($Zn_{0.94}Co_{0.06}O$) window layer, designed to improve light absorption and carrier transport. This structure has the same characteristics as Figure 1 except that we have replaced the ZnO layer with $Zn_{0.94}Co_{0.06}O$.

3. RESULTS EXPLANATION

In this section, we present and discuss the results of the performance analysis of Concentrated Solar Photovoltaic (CSPV) cells incorporating ZnO and cobalt-doped ZnO ($Zn_{0.94}Co_{0.06}O$) as window layers. The primary objective of this analysis is to investigate how cobalt incorporation into the ZnO matrix influences the photovoltaic parameters and overall efficiency of the cells. Key performance indicators evaluated include the open-circuit voltage (V_{oc}), short-circuit current density (J_{sc}), fill factor (FF), and power conversion efficiency (PCE). By comparing the performance metrics of cells using undoped ZnO versus those employing $Zn_{0.94}Co_{0.06}O$, we aim to determine the extent to which Co doping enhances the optoelectronic properties of the window layer. The results reveal that the inclusion of cobalt leads to improved light absorption, reduced carrier recombination, and enhanced charge transport, all of which contribute to significant gains in device performance. Thus, $Zn_{0.94}Co_{0.06}O$ emerges as a promising alternative to conventional ZnO, offering superior energy conversion efficiency in CSPV cell applications.

3.1 Results the CSPV Cell with ZnO Window Layer

3.1.1 Analysis of I(V) Characteristics for ZnO/GaSb/GaSbBi(3 %)/GaAsSbBi/GaSbBi (6 %)/GaAs Structure

The $I(V)$ characteristic curve in Figure 3 illustrates the relationship between voltage (V) and current density (I) for a CSPV cell with the ZnO/GaSb/GaSbBi (3 %)/GaAsSbBi/GaSbBi (6 %)/GaAs structure. This analysis focuses on understanding how doping concentrations influence the photovoltaic performance of this structure.

The curve shows an exponential increase in current density as the voltage rises, which is typical of a diode-like behavior in photovoltaic cells. As observed, the current density remains relatively low at lower voltage levels, then increases significantly as the voltage approaches the open-circuit condition. This behavior aligns with the theory that higher dopant concentrations in the absorber layers can enhance charge carrier collection and transport properties within the cell [11].

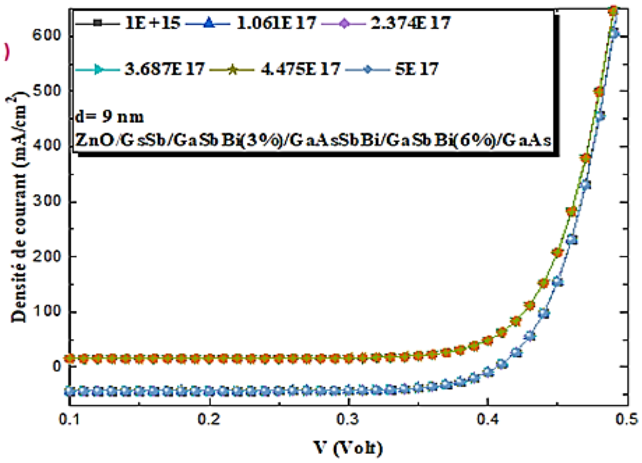

Fig. 3 – The I(V) Characteristic of ZnO/GaSb/GaSbBi (3 %)/GaAsSbBi/ GaSbBi (6 %)/GaAs

The different doping concentrations noted by values such as 1×10^{15} to 5×10^{17} cm^{-3} significantly affect the current density. At lower doping concentrations, the current density remains modest due to limited charge carriers in the semiconductor layers, which hinders efficient electron-hole pair generation and collection. However, as the doping concentration increases, we observe a higher current density, indicating that the enhanced carrier concentration facilitates more effective absorption and transport of photo-generated electrons. Studies have shown that doping semiconductor layers with higher concentrations of elements like bismuth and arsenic in GaSb-based structures can result in improved electrical conductivity and absorption characteristics, thus boosting current density.

The inclusion of GaSbBi and GaAsSbBi layers, with varying bismuth concentrations (3 % and 6 %), plays a crucial role in extending the absorption range into the infrared spectrum. This is especially relevant for concentrated solar photovoltaic applications, as the broader absorption spectrum enables the cell to capture more photons and increase the overall current output [12]. The enhanced absorption in the infrared region helps maintain higher current densities at different voltages, contributing to overall improved efficiency.

The exponential rise in current density with increasing voltage highlights the effectiveness of the ZnO/GaSb/GaSbBi structure in capturing and converting solar energy at high concentration levels. At high doping levels (e.g., 5×10^{17} cm^{-3}), the current density reaches its peak due to the optimized balance between absorption and charge carrier transport. This performance indicates a reduction in recombination losses, which is a known challenge in highly doped materials. Improved current density with increased doping concentration suggests that the Co-doped ZnO layer supports effective charge extraction, as observed in similar studies on ZnO-based photovoltaic cells.

In summary, the *I*(*V*) characteristics of this CSPV structure demonstrate that higher doping levels in GaSbBi and GaAsSbBi layers significantly enhance current density and overall photovoltaic performance. The results support the hypothesis that Co-doped ZnO, in conjunction with GaSbBi and GaAsSbBi layers, optimizes light absorption and charge transport. This combination creates an efficient pathway for photovoltaic conversion, providing valuable insights into the design of high-performance CSPV cells.

3.1.2 Analysis of V_{oc} and J_{sc} Variation with Shallow Acceptor Density

The graph above illustrates the variation of open-circuit voltage (V_{oc}) and short-circuit current density (J_{sc}) as a function of shallow acceptor density in a CSPV structure composed of GaSb/GaSbBi(3 %)/GaAsSbBi /GaSbBi(6 %)/GaAs with a 9 nm Co-doped ZnO window layer. Both parameters, V_{oc} (in black) and J_{sc} (in red), are plotted against the shallow acceptor density (1/cm^3).

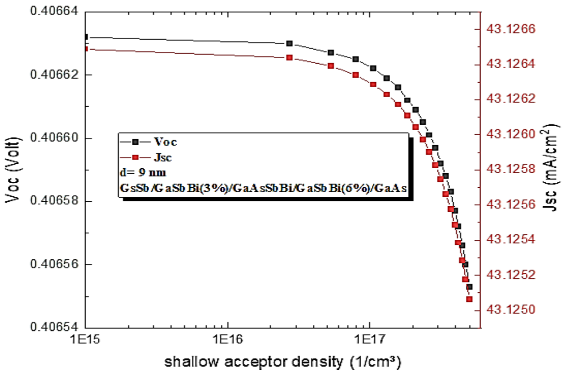

Fig. 4 – Variation of (a) V_{oc} and J_{sc} as a function of GaSbBi (6 %) doping concentration

The open-circuit voltage V_{oc} shows a slight decrease as the shallow acceptor density increases, starting from approximately 0.40664 V at lower densities around 1×10^{15} cm – 3.1×10^{15} cm^{-3} and gradually decreasing as the density reaches 1×10^{17} cm – 3.10^{17} cm^{-3}. This decrease in V_{oc} is consistent with previous studies that demonstrate an inverse relationship between doping concentration and open-circuit voltage in semiconductor materials [13]. Higher acceptor densities can increase recombination rates in the cell, leading to a reduction in Voc due to the increased probability of charge carriers recombining before contributing to the electric current.

Similarly, the short-circuit current density J_{sc} shows a slight decline as the acceptor density increases, from approximately 43.1266 mA/cm^2 to 43.1250 mA/cm^2. Although the variation is minor, it suggests that higher acceptor densities may slightly hinder the transport of photogenerated carriers. This is likely due to increased internal electric field screening effects, where a higher density of acceptors can weaken the internal electric field that aids in carrier collection, leading to marginal decreases in J_{sc} [14].

The observed trends in V_{oc} and J_{sc} with respect to shallow acceptor density provide insights into the optimal doping levels for CSPV cells. While higher acceptor densities can enhance conductivity, they also introduce more recombination centers, potentially limiting both V_{oc} and J_{sc}. Thus, balancing acceptor density is crucial for achieving optimal efficiency in CSPV cells. Keeping the acceptor density within a moderate range can help maintain both high V_{oc} and J_{sc}, supporting efficient solar conversion [15].

In conclusion, both Voc and Jsc show a slight decline with increasing shallow acceptor density in the GaSb-based CSPV cell. These findings highlight the importance of optimizing doping levels to minimize recombination while maintaining effective carrier transport. This balance is key to maximizing the performance of CSPV cells, especially in structures using Co-doped ZnO as a window layer and GaSb-based absorbers, which are designed for high-efficiency applications [16].

3.1.3 Analysis of FF and Efficiency (η\eta$\eta$) Variation with Shallow Acceptor Density

The graph above shows how the Fill Factor (FF) and efficiency (η) of a CSPV cell with a structure of GaSb/GaSbBi (3 %)/GaAsSbBi/GaSbBi (6 %)/GaAs and a 9 nm Co-doped ZnO window layer vary with increasing shallow acceptor density (1/cm^3).

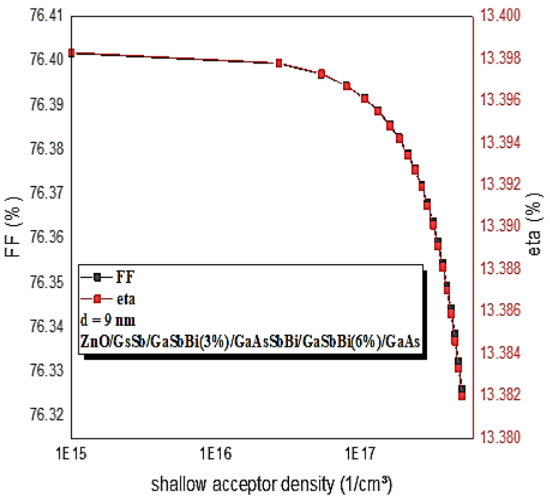

Fig. 5 – Variation of FF and Efficiency (η) as a function of GaSbBi (6 %) doping concentration

The Fill Factor (FF) remains relatively stable at around 76.40 % for lower acceptor densities, specifically between 1×10^{15} and $1 \times 10^{16}\,\text{cm}^{-31}$, $1 \times 10^{16}\,\text{cm}^{-3}$. However, as the shallow acceptor density increases beyond this range, a slight decline in FF is observed, dropping to approximately 76.32 % at the highest density values. This decrease is likely due to increased recombination rates associated with higher doping levels, which reduce the efficiency with which the cell converts available charge carriers into usable current [5]. Elevated recombination lowers the maximum power point, impacting the FF and thus the overall performance of the cell.

Similarly, the efficiency (η\eta$\eta$) of the cell initially shows stability at lower acceptor densities, maintaining a value around 13.40 %. However, as the shallow acceptor density increases, the efficiency starts to drop slightly, reaching approximately 13.382 % at the highest acceptor densities. This reduction in efficiency is consistent with the trend observed in FF, as higher recombination rates and decreased carrier lifetime negatively affect the energy conversion process [17]. High doping levels can introduce additional defects or recombination centers within the material, thus limiting the effective carrier transport and lowering the overall efficiency [18].

The data suggest that there is an optimal range of shallow acceptor density where both FF and efficiency remain relatively high. Keeping the acceptor density below $1 \times 10^{17}\,\text{cm} - 3.1 \times 10^{17}\,\text{cm}^{-3}$ seems to be beneficial in maintaining the cell's performance. Beyond this threshold, the adverse effects of excessive doping, such as increased recombination and diminished carrier mobility, start to outweigh the benefits, leading to reduced FF and efficiency. Finding this balance in doping concentration is crucial to optimize CSPV cell performance [19].

In summary, this analysis indicates that while shallow acceptor density can enhance certain properties of the cell, excessive doping results in a decline in both FF and efficiency due to increased recombination. For optimal performance, maintaining a moderate doping concentration is essential to balance carrier generation and transport without incurring significant recombination losses.

3.1.4 Analysis of V_{oc} and J_{sc} Variation with GaSbBi (6 %) Layer Thickness

The graph illustrates how the open-circuit voltage (V_{oc}) and short-circuit current density (J_{sc}) vary as the thickness ddd of the GaSbBi (6 %) layer changes in a CSPV cell with the structure ZnO/GaSb/GaSbBi(3 %)/GaAsSbBi/GaSbBi(6 %) /GaAs and a specified acceptor concentration ($N_A = 3.50 \times 10^{16}\,\text{cm}^{-3}$).

As the GaSbBi (6 %) layer thickness increases, both V_{oc} and J_{sc} demonstrate a gradual decrease, revealing important insights about the behavior of the cell's efficiency under varying material thicknesses. The GaSbBi (6 %) layer, which is doped with 6 % bismuth to broaden the light absorption range, plays a significant role in determining how effectively the cell converts sunlight into electrical energy. A thicker GaSbBi (6 %) layer allows for more light absorption; however, it also introduces additional challenges. With increased thickness, the path for photogenerated carriers (electrons and holes) becomes longer, which can lead to a higher probability of recombination losses. This, in turn, reduces the open-circuit voltage (V_{oc}), as fewer charge carriers reach the junction to contribute to the voltage across the cell.

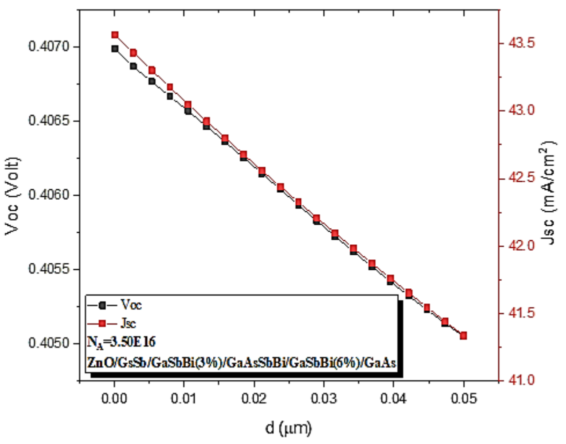

Fig.6 – Variation of V_{oc} and J_{sc} Variation with GaSbBi (6%) layer thickness

The open-circuit voltage V_{oc} shows a gradual decrease as the thickness of the GaSbBi (6 %) layer increases, starting from approximately 0.4070 V at very thin layers and dropping to around 0.4050 V at a thickness of 0.05 μm. This reduction in V_{oc} with increased thickness can be attributed to higher recombination rates in thicker layers, which reduce the effective voltage. As the thickness increases, the path for charge carriers becomes longer, potentially leading to more recombination events before they reach the electrodes, which lowers the overall V_{oc} [5].

Similarly, the short-circuit current density J_{sc} also declines as the GaSbBi (6 %) layer thickness increases. Starting from approximately 43.5 mA/cm^2 at thinner layers, it gradually drops to about 41.0 mA/cm^2 at the highest thickness. This behavior is likely due to increased optical absorption in thicker layers, which can cause more photon absorption but may also introduce more recombination centers, leading to a decrease in the effective collection of carriers [20]. Additionally, as the layer thickens, internal resistances increase, which can inhibit efficient carrier transport, further reducing J_{sc} [21].

The data indicate that there is an optimal thickness for the GaSbBi (6 %) layer, where both V_{oc} and J_{sc} remain relatively high. Extremely thin layers may not capture enough light, resulting in lower J_{sc}, while overly thick layers increase recombination and resistance, decreasing both V_{oc} and J_{sc}. This suggests that a moderate thickness, likely in the range of a few tens of nanometers, may yield the best balance between light absorption and carrier collection efficiency [22].

In summary, both V_{oc} and J_{sc} decline with increasing thickness of the GaSbBi (6 %) layer. This trend highlights the importance of carefully optimizing layer thickness to minimize recombination and resistance effects while maximizing photon absorption and carrier transport. Finding an optimal thickness is crucial for enhancing CSPV cell performance, especially in cells with multi-layer structures designed for high-efficiency energy conversion.

3.1.5 Analysis of FF and Efficiency (η) Variation with GaSbBi (6 %) Layer Thickness

The graph illustrates how the Fill Factor (FF) and efficiency (η) of a Concentrated Solar Photovoltaic (CSPV) cell vary as the thickness (d) of the GaSbBi (6 %) layer increases. This CSPV cell structure consists of multiple layers, including ZnO/GaSb/GaSbBi(3 %)/GaAsSbBi/GaSbBi(6 %)/GaAs, with an acceptor concentration ($N_A = 3.50 \times 10^{16}$ cm^{-3}) that contributes to the formation of charge carriers in the cell. Each layer in this multi-layer structure is carefully engineered to optimize light absorption and carrier transport, with the GaSbBi (6 %) layer specifically tailored to absorb a broader range of wavelengths, particularly in the infrared region. As the thickness of this layer increases, it enhances the cell's ability to capture more photons, which theoretically should boost the efficiency.

The Fill Factor (FF) exhibits a gradual decline as the thickness of the GaSbBi (6 %) layer increases. Starting from a higher value of around 76.4 % for thinner layers, the FF drops steadily, reaching approximately 75.9 % at a thickness of 0.05 μm. This decline can be attributed to the impact of increased layer thickness on internal resistance and carrier recombination. As the GaSbBi layer becomes thicker, the distance that charge carriers must travel to reach the junction increases, making it more likely for recombination to occur. This recombination reduces the effective charge carriers contributing to current, thereby lowering the FF [23]. Additionally, thicker layers may also introduce higher series resistance within the cell, further impacting the FF as it affects the maximum power output [24].

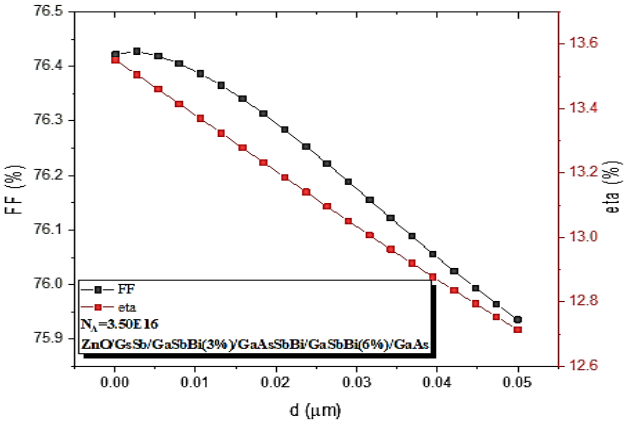

Fig. 7 – Variation of FF and Efficiency (η\eta$\eta$) as a Function of GaSbBi (6 %) layer thickness

The efficiency (η\eta$\eta$) of the cell, shown by the red curve, follows a similar downward trend as the GaSbBi (6 %) layer thickness increases. Starting from around 13.6 % at thinner layers, the efficiency decreases progressively, dropping to approximately 12.6 % at a thickness of 0.05 μm. This reduction in efficiency can be explained by the combined effects of increased recombination and internal resistance as the GaSbBi layer becomes thicker. While a thicker GaSbBi layer does enhance light absorption due to a larger volume for photon interaction, the downside is that the generated electron-hole pairs are more likely to recombine before contributing to the current, reducing the overall efficiency [24].

The declining efficiency trend suggests that there is a point beyond which additional thickness in the GaSbBi layer is detrimental to the cell's performance. At this point, the negative impact of recombination and resistance outweighs the benefits of enhanced light absorption. This observation aligns with findings from similar studies, where the optimization of layer thickness is critical for balancing absorption and carrier transport.

The data from this graph indicate that an optimal thickness exists for the GaSbBi (6 %) layer, where both FF and efficiency are maximized before the adverse effects of recombination and resistance become dominant. A moderate thickness would likely yield a balance, capturing sufficient light while maintaining effective charge transport. This balance is essential in CSPV cells with complex multi-layer structures like this one, where each layer's thickness can impact overall performance [25].

In summary, both the Fill Factor (FF) and efficiency (η\eta$\eta$) decrease with increasing GaSbBi (6 %) layer thickness, suggesting a trade-off between light absorption and charge carrier collection. Finding the optimal thickness for the GaSbBi (6 %) layer is crucial for achieving high performance in CSPV cells, ensuring that recombination and resistance are minimized while absorption remains effective.

3.1.6 Analysis of External Quantum Efficiency (EQE) Variation with GaSbBi (6 %) Layer Thickness

The graph illustrates the External Quantum Efficiency (EQE) response of a Concentrated Solar Photovoltaic (CSPV) cell featuring a multilayered heterostructure composed of GaSb/GaSbBi(3 %)/GaAsSbBi/GaSbBi(6 %)/GaAs, evaluated over a broad spectral range extending from approximately 300 nm to 1800 nm. The analysis focuses on the influence of varying the thickness of the GaSbBi layer with 6 % bismuth content, examining values from 0.0001 µm to 0.032 µm. This variation is intended to assess how the thickness of the Bi-rich absorber layer affects photon absorption and carrier collection efficiency. The acceptor doping concentration is maintained at a constant value of $ND = 3.5 \times 10^{16}$ cm^{-3}, which plays a critical role in defining the depletion region width, electric field distribution, and carrier transport characteristics within the junction. By analyzing the EQE behavior as a function of both wavelength and GaSbBi(6 %) layer thickness, the study aims to identify the optimal configuration that maximizes photocarrier generation and overall spectral response of the device.

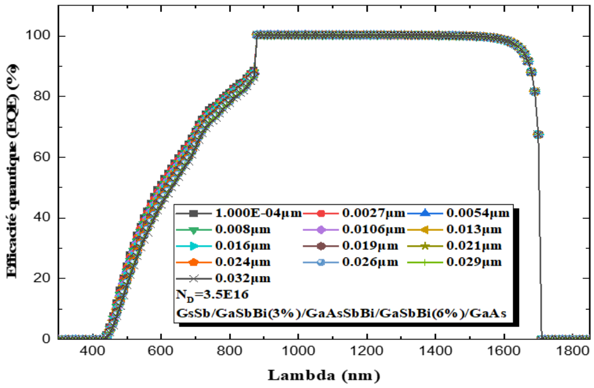

Fig. 8 – External Quantum Efficiency (EQE) of the GaSb/GaSbBi (3 %)/GaAsSbBi/GaSbBi (6 %)/GaAs structure as a function of wavelength for different thicknesses of the GaSbBi (6 %) layer

In the wavelength range from around 400 nm to 1000 nm, the EQE rises steeply and reaches a peak close to 100 %. This indicates that the cell performs effectively within this range, with high photon absorption and efficient conversion of incident light into charge carriers. This high EQE in the visible spectrum aligns with the cell's design, as the GaSbBi (6 %) and GaAsSbBi layers are optimized to capture and convert photons within this range [26].

The different GaSbBi (6 %) layer thicknesses show minimal variation in EQE values, especially within the high-efficiency region (400 nm to 1000 nm). This suggests that within this wavelength range, variations in the GaSbBi layer thickness do not significantly impact the cell's ability to absorb photons and generate charge carriers. This stability in EQE performance can be beneficial in practical applications, where slight deviations in layer thickness might occur during fabrication [27]. However, at wavelengths beyond 1000 nm, slight variations in EQE are observed across different thicknesses, indicating that thicker layers might provide slightly enhanced absorption in the near-infrared range, though the overall effect remains limited.

As the wavelength extends beyond 1000 nm and into the near-infrared region, the EQE begins to decrease for all thicknesses, eventually approaching zero at around 1800 nm. This decline is expected, as the materials in the GaSbBi and GaAsSbBi layers have limited absorption capabilities in this part of the spectrum. Despite some marginal improvements with increased thickness, the EQE remains relatively low beyond 1000 nm, suggesting that this structure primarily targets the visible to near-infrared range for optimal efficiency [28].

The data from this graph indicate that, for maximizing EQE, the GaSbBi (6 %) layer thickness does not need to be excessively thick, as increased thickness beyond a certain point offers limited benefits in the visible range. This finding suggests that a moderate thickness is sufficient for effective photon absorption and charge generation, allowing for material savings without compromising performance. However, slight thickness adjustments could be beneficial for optimizing absorption in the longer wavelengths within the near-infrared region, though the gains may be minimal [28].

In summary, the EQE of the GaSb/GaSbBi (3 %) /GaAsSbBi/GaSbBi (6 %)/GaAs structure shows high efficiency in the 400 nm to 1000 nm range, with minimal variation across different GaSbBi (6 %) layer thicknesses. This consistency indicates that moderate layer thickness is sufficient for effective photon absorption and conversion, while thicker layers may provide minor improvements in the near-infrared. Optimizing the GaSbBi (6 %) thickness for high EQE in the visible spectrum can enhance CSPV cell performance without unnecessary material use, supporting efficient and cost-effective cell design.

3.2 Results the CSPV Cell with ZnCoO Window Layer

3.2.1 Analysis of *I*(*V*) Characteristics for ZnCoO/ GaSb/GaSbBi(3 %)/GaAsSbBi/GaSbBi (6 %)/GaAs Structure

Figure 8 shows the *I*(*V*) characteristic curves for a CSPV cell with the structure GaSb/GaSbBi (3 %)/GaAsSbBi/GaSbBi (6 %)/GaAs/ZnCoO at various ZnCoO doping concentrations. The x-axis represents the voltage (*V*), while the *y*-axis shows the current density (*J*) in mA/cm^2. As the doping concentration of ZnCoO increases from 1×10^{16} to 5×10^{17} cm^{-3}, a noticeable rise in current density is observed, particularly at higher voltage levels.

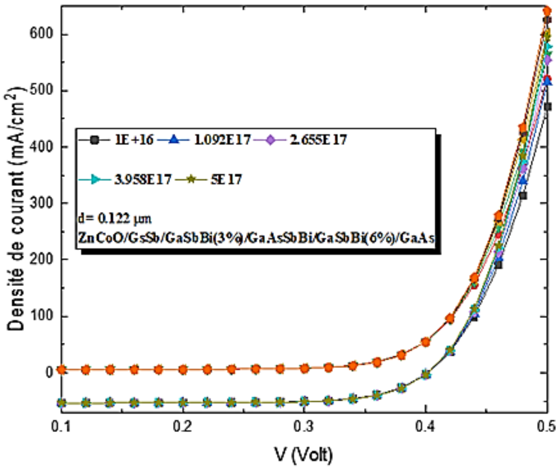

Fig. 9 – The $I(V)$ Characteristic of ZnCoO/GaSb/GaSbBi (3 %)/GaAsSbBi/GaSbBi(6 %)/GaAs

The progressive increase in current density observed with higher levels of cobalt doping in the ZnO layer highlights a significant enhancement in the optoelectronic properties of the material. This improvement is primarily attributed to enhanced photogeneration and more efficient transport of charge carriers. As cobalt atoms are introduced into the ZnO lattice, they modify the band structure by creating intermediate energy states that expand light absorption into the visible range, thereby increasing the number of photogenerated electron-hole pairs. Moreover, Co doping tends to increase the carrier concentration and reduce the resistivity of the ZnO layer, which promotes faster and more efficient transport of electrons towards the cathode and holes towards the anode. Simultaneously, cobalt helps passivate intrinsic defects, such as oxygen vacancies, which are known to act as non-radiative recombination centers. This leads to a notable reduction in recombination losses. These combined effects culminate in a marked rise in current density, especially at forward voltages approaching 0.5 V, where charge extraction is most active. This behavior underscores the role of ZnCoO as a highly promising window or buffer layer in compound semiconductor photovoltaic (CSPV) cells, effectively boosting the overall energy conversion efficiency of the device.

3.2.2 Analysis of the Effect of ZnCoO Doping on V_{oc}, J_{sc}, FF, and Efficiency (η)

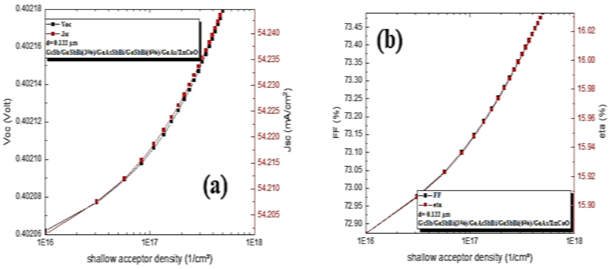

Fig. 10 – Two subplots analyzing the impact of ZnCoO doping concentration on key photovoltaic parameters in a CSPV cell structured as ZnCoO/GaSb/GaSbBi (3 %)/GaAsSbBi/GaSbBi (6 %)/GaAs.

3.2.2.a Subplot (a): This graph shows the variation of open-circuit voltage (V_{oc}) and short-circuit current density (J_{sc}) as functions of shallow acceptor density ZnCoO doping concentration. Both V_{oc} and J_{sc} increase with higher doping levels. The rise in V_{oc} indicates enhanced carrier. Parathion, likely due to improved electric fields within the device structure. Similarly, the increase in J_{sc} suggests better photon absorption and carrier generation, as higher doping enhances conductivity, allowing more efficient current flow [29].

3.2.2.b Subplot (b): This graph illustrates the changes in Fill Factor (FF) and efficiency (η) with increasing ZnCoO doping concentration. Both FF and efficiency show a positive trend, with values rising consistently as doping concentration increases. This enhancement can be attributed to reduced recombination rates and improved carrier mobility, resulting from the optimized electronic properties introduced by Co-doping in the ZnO layer. Higher doping concentrations allow the cell to reach optimal power output, thus improving FF and efficiency [30].

Tabel 1 – Comparison of electrical performance parameters for CSPV structures with ZnO and Co-doped ZnO window layers

	Structure 1 ZnO	Structure 2 Co-doped ZnO
Incident power on solar cell structure (W/m^2)	1000	1000
V_{oc} (V)	0.41	0.402
Jsc (mA/cm^{-2})	43.43	54.20
FF%	76.42	72.90
Yield	13.55 %	15.89 %

The theoretical study evaluates the potential impact of using ZnO and Co-doped ZnO as window layers in CSPV structures, focusing on key electrical performance parameters such as open-circuit voltage (V_{oc}), short-circuit current density (J_{sc}), fill factor (FF), and overall efficiency.

The theoretical analysis suggests that incorporating Co-doped ZnO could lead to significant enhancements in photovoltaic performance. For instance, the short-circuit current density (J_{sc}) is predicted to increase from 43.43 mA/cm^2 for pure ZnO to 54.20 mA/cm^2 for Co-doped ZnO. This improvement is attributed to the enhanced optical and electrical properties of Co-doped ZnO, which is expected to facilitate better light absorption and improved charge carrier collection.

The open-circuit voltage (V_{oc}) for the Co-doped ZnO structure shows a slight decrease, with a value of 0.402 V compared to 0.41 V for ZnO. Despite this minor reduction, the impact on overall performance is minimal, as the efficiency gains from other parameters outweigh this loss. Additionally, the fill factor (FF) for Co-doped ZnO is theoretically predicted to be slightly lower at 72.90 % compared to 76.42 % for ZnO. This could be due to an increase in series resistance or other losses introduced by the doping process.

Most importantly, the theoretical efficiency analysis indicates a significant improvement when using Co-doped ZnO. The efficiency increases from 13.55 % for the ZnO-based structure to 15.89 % for the Co-doped ZnO structure. This improvement highlights the potential of Co-doped ZnO to optimize energy conversion, thanks to its superior ability to enhance both optical and electrical performance.

CONCLUSION

The theoretical findings suggest that Co-doped ZnO offers promising advantages as a window layer material in CSPV structures. While minor trade-offs in V_{oc} and FF are observed, the notable improvements in J_{sc} and overall efficiency position Co-doped ZnO as a superior alternative to pure ZnO. These results underscore the importance of material innovation in the pursuit of higher-performing photovoltaic technologies.

REFERENCES

1. F. Bouhjar, B. Marí, L. Derbali, *Nano Res.* **13** No 9, 2546 (2020).
2. S. Tayyaba, V.E. Balas, M.I. Tariq, M.M. Balas, M.W. Ashraf, M. Akhlaq, N. Wang, *Energies* **13** No 18, 4863 (2020).
3. J.J. Cole, H. Jacobs, *MRS Proceedings* **1192**, 1 (2009).
4. B. Panigrahy, D. Bahadur, M. Aslam, *J. Phys. Chem. C* **114** No 27, 11758 (2010).
5. O. Delorme, E. Tournié, J.-B. Rodriguez, M. Gladysiewicz, L. Cerutti, J. Kopaczek, R. Kudrawiec, E. Luna, A. Trampert, *GaSbBi Alloys and Heterostructures: Fabrication and Properties.* In *Bismuth-Containing Alloys and Nanostructures*, **285**, 125 (Eds. by S. Wang, P. Lu) (Springer Series in Materials Science: Springer, Singapore: 2019).
6. Ö. Çelik, Ş. Baturay, Y.S. Ocak, *Mater. Res. Exp.* **7** No 2, 026403 (2020).
7. M.Z. Alotaibi, A. Merazga, B.M. Omer, S. Alomairy, *AIP Conf. Proc.* **1976** No 1, 020010 (2018).
8. J. Wojnarowicz, W. Lojkowski, K. Sobczak, T. Chudoba, S. Gierlotka, *Crystals* **8** No 4, 179 (2018).
9. S. Antohe, C. Tazlaoanu, I. Enculescu, G. Socol, D. Bazavan, L. Magherusan, I. Mihailescu, *MRS Proceedings*, **1013**, 409 (2007).
10. K. Kakimoto, *Czochralski Silicon Single Crystals for Semiconductor and Solar Cell Applications* In *Springer Handbook of Crystal Growth*, 231 (Eds. by G. Dhanaraj, K. Byrappa, V. Prasad, M. Dudley) (Springer Handbooks. Springer: Berlin, Heidelberg: 2010).
11. C. Jin, S. Nori, R.J. Narayan, W. Wei, D. Kumar, R. Aggarwal, *J. Nanosci. Nanotechnol.* **8** No 11, 6043 (2008).
12. C. Wang, Z. Zhang, *AIP Adv.* **11** No 2, 025107 (2021).
13. R. Podila, S.S.S. Sai, J. He, A.M. Rao, R. Philip, M. Skove, B. Anand, J.P. West, S.-J. Hwu, S. Tewari, *Nanotechnology* 22 No 9, 095703 (2011).
14. I. Djerdj, M. Niederberger, D. Arčon, Z. Jagličić, *Nanoscale* **2** No 7, 1096 (2010).
15. P. Potera, B. Cieniek, I.S. Virt, *Appl. Sci.* **13** No 4, 2701 (2023).
16. W.-Z. Yang, I. Ullah, Z.-G. Jiang, R.B. Neder, C.-H. Zhan, *RSC Adv.* **15** No 15, 11934 (2025).
17. O. Delorme, G. Narcy, E. Luna, A. Trampert, E. Tournié, J.-B. Rodriguez, L. Cerutti, *Appl. Phys. Lett.* **110** No 22, 222106 (2017).
18. M. Osawa, *Surface-Enhanced Infrared Absorption Spectroscopy* In *Compendium of Surface and Interface Analysis*, 697 (Eds. by *The Surface Science Society of Japan*) (Springer: Singapore: 2018).
19. C. Rao, F. Deepak, https://arxiv.org/pdf/cond-mat/0407108 (2004).
20. Y. Wang, L. Sun, D.-D. Han, R.-Q. Han, Y. Li, L.-F. Liu, X. Zhang, Y.-F. Zhang, J.-F. Kang, *2007 International Conference on Solid State Devices and Materials* (Ibaraki, Japan: 2007).
21. R. Schneider, L.D. Yao, D. Gerthsen, G. Mayer, M. Fonin, U. Rüdiger, *Structural and Chemical Characterization of Co-doped ZnO Layers Grown on Si and Sapphire* In *EMC 2008 14th European Microscopy Congress*, 621 (Eds. by S. Richter, A. Schwedt) (Aachen, Germany: Springer, Berlin, Heidelberg: 2008).
22. Z. Cao, T. Veal, M. Ashwin, I. Sandall, *2020 IEEE Photonics Conference (IPC)* (IEEE: 2020).
23. A. Saad, N. Hamad, R.A.F. Redoy, S. Zhao, S. Wageh, *Polymers* **16** No 16, 2347 (2024).
24. K. Jarašiūnas, V. Soukhoveev, T. Malinauskas, V. Gudelis, S. Nargelas, J.V. Vaitkus, A. Usikov, *phys. status solidi b* **247** No 7, 1703 (2010).
25. A. Kumar, S. Singh, R. Kumar, *Optimization of Charge Transport Layer Thickness for Efficient Perovskite Solar Cell* In *Recent Advances in Power Electronics and Drives. Lecture Notes in Electrical Engineering*, **707**, 193 (Eds. by J. Kumar, P. Jena) (Springer, Singapore: 2020).
26. L. Bonderer, P. Smith, W. Caseri, D. Uhlenhaut, *Materials (Basel, Switzerland)*, **7** No 3, 1899 (2014).
27. H. Jiang, V.A. Kildishev, W. Zhu, J. Huang, Y. Wang, *Photonics* **11** No 10, 917 (2024).
28. H. Aiki, T. Yamagata, *Ocean Sci.* **2** No 2, 161 (2006).
29. M. Hayashi, Y. Okuzu, B. Otsuki, S. Yamaguchi, T. Shimizu, T. Kawai, S. Fujibayashi, M. Imamura, S. Matsuda, K. Goto, *Sci. Rep.* **11**, 15875 (2021).
30. G.M. Smith, J.S. Flynn, J.M. Redwing, R.P. Vaudo, J.W. Szewczuk, V.M. Phanse, K.S. Boutros, *Proc. SPIE* **3279**, Light-Emitting Diodes: Research, Manufacturing, and Applications II (1998).

Покращення ефективності концентраційної сонячної фотографічної системи (CSPV) за допомогою легованих шарів ZnO та підкладок GaSb, насичених Bi-As

Charef Azzeddine[1,2], Karima Zitouni[1], Said Benramache[2], Khattra Mimouni[1], Abderrahmane Kadri[1]

[1] *LEMOP Laboratory, Laboratoire d'Etude des Matériaux Optoélectronique et Polymères, University Oran*1*, Algeria*
[2] *Laboratoire de Physique Photonique et Nanomatériaux Multifonctionnels, LPPNM, Biskra University, Algeria*

Робота присвячена дослідженню покращення продуктивності концентраційних сонячних фотографічних модулів (CSPV) за допомогою оптимізованих окисних шарів та унікального субстрату GaSb, насиченого сполуками миш'яку-арсену (Bi-As), для підвищення перетворення сонячної енергії. Було вивчено дві конфігурації: одну з чистим віконним шаром ZnO та іншу з Co-допованим ZnO ($Zn_{0.94}Co_{0.06}O$). Обидва модулі містили шар GaSb, насичений 3 % та 6 % Bi у GaSbBi та GaAsSbBi відповідно, з метою збільшення поглинання світла. Результати показують істотне збільшення ефективності у модулі з віконним шаром $Zn_{0.94}Co_{0.06}O$, що демонструє його переваги порівняно з модулем на основі ZnO незалежно від товщини шару GaAsSbBi. Модуль CSPV з ZnO досягнув коефіцієнта перетворення енергії 13,55 % та коефіцієнта заповнення (FF) 76,42 %. У порівнянні з цим, Co-допований ZnO ($Zn_{0.94}Co_{0.06}O$) суттєво покращив ефективність, досягнувши 15,89 % при FF 72,90 %. Це збільшення вихідної потужності підкреслює ефективність Co-допованого ZnO як просунутого віконного шару, що стабільно підвищує ефективність перетворення енергії у різних товщинах шару GaAsSbBi. Результати свідчать, що шар з Co-допованим ZnO є перспективним підходом для оптимізації CSPV-модулів, що робить його цінним розвитком для підвищення фотогальванічної ефективності та сприяє більш стабільним рішенням у галузі сонячної енергетики.

Ключові слова: CSPV модулі, Спільно леговані підкладки ZnO, GaSbBi, Оптимізація сонячної ефективності.